DESY–08–132
December 2008

A measurement of the Q^2, W and t dependences of deeply virtual Compton scattering at HERA

ZEUS Collaboration

Abstract

Deeply virtual Compton scattering, $\gamma^* p \to \gamma p$, has been measured in $e^+ p$ collisions at HERA with the ZEUS detector using an integrated luminosity of 61.1 pb^{-1}. Cross sections are presented as a function of the photon virtuality, Q^2, and photon-proton centre-of-mass energy, W, for a wide region of the phase space, $Q^2 > 1.5$ GeV^2 and $40 < W < 170$ GeV. A subsample of events in which the scattered proton is measured in the leading proton spectrometer, corresponding to an integrated luminosity of 31.3 pb^{-1}, is used for the first direct measurement of the differential cross section as a function of t, where t is the square of the four-momentum transfer at the proton vertex.

The ZEUS Collaboration

S. Chekanov, M. Derrick, S. Magill, B. Musgrave, D. Nicholass[1], J. Repond, R. Yoshida
Argonne National Laboratory, Argonne, Illinois 60439-4815, USA [n]

M.C.K. Mattingly
Andrews University, Berrien Springs, Michigan 49104-0380, USA

P. Antonioli, G. Bari, L. Bellagamba, D. Boscherini, A. Bruni, G. Bruni, G. Cara Romeo
F. Cindolo, M. Corradi, G. Iacobucci, A. Margotti, T. Massam, R. Nania, A. Polini
INFN Bologna, Bologna, Italy [e]

S. Antonelli, M. Basile, M. Bindi, L. Cifarelli, A. Contin, F. Palmonari, S. De Pasquale[2],
G. Sartorelli, A. Zichichi
University and INFN Bologna, Bologna, Italy [e]

D. Bartsch, I. Brock, H. Hartmann, E. Hilger, H.-P. Jakob, M. Jüngst, A.E. Nuncio-Quiroz,
E. Paul, U. Samson, V. Schönberg, R. Shehzadi, M. Wlasenko
Physikalisches Institut der Universität Bonn, Bonn, Germany [b]

N.H. Brook, G.P. Heath, J.D. Morris
H.H. Wills Physics Laboratory, University of Bristol, Bristol, United Kingdom [m]

M. Kaur, P. Kaur[3], I. Singh[3]
Panjab University, Department of Physics, Chandigarh, India

M. Capua, S. Fazio, A. Mastroberardino, M. Schioppa, G. Susinno, E. Tassi
Calabria University, Physics Department and INFN, Cosenza, Italy [e]

J.Y. Kim
Chonnam National University, Kwangju, South Korea

Z.A. Ibrahim, F. Mohamad Idris, B. Kamaluddin, W.A.T. Wan Abdullah
Jabatan Fizik, Universiti Malaya, 50603 Kuala Lumpur, Malaysia [r]

Y. Ning, Z. Ren, F. Sciulli
Nevis Laboratories, Columbia University, Irvington on Hudson, New York 10027 [o]

J. Chwastowski, A. Eskreys, J. Figiel, A. Galas, K. Olkiewicz, B. Pawlik, P. Stopa,
L. Zawiejski
*The Henryk Niewodniczanski Institute of Nuclear Physics, Polish Academy of Sciences,
Cracow, Poland* [i]

L. Adamczyk, T. Bołd, I. Grabowska-Bołd, D. Kisielewska, J. Łukasik[4], M. Przybycień,
L. Suszycki
*Faculty of Physics and Applied Computer Science, AGH-University of Science and Technology,
Cracow, Poland* [p]

A. Kotański[5], W. Słomiński[6]
Department of Physics, Jagellonian University, Cracow, Poland

O. Behnke, U. Behrens, C. Blohm, A. Bonato, K. Borras, D. Bot, R. Ciesielski, N. Coppola, S. Fang, J. Fourletova[7], A. Geiser, P. Göttlicher[8], J. Grebenyuk, I. Gregor, T. Haas, W. Hain, A. Hüttmann, F. Januschek, B. Kahle, I.I. Katkov[9], U. Klein[10], U. Kötz, H. Kowalski, M. Lisovyi, E. Lobodzinska, B. Löhr, R. Mankel[11], I.-A. Melzer-Pellmann, S. Miglioranzi[12], A. Montanari, T. Namsoo, D. Notz[11], A. Parenti, L. Rinaldi[13], P. Roloff, I. Rubinsky, U. Schneekloth, A. Spiridonov[14], D. Szuba[15], J. Szuba[16], T. Theedt, J. Ukleja[17], G. Wolf, K. Wrona, A.G. Yagües Molina, C. Youngman, W. Zeuner[11]
Deutsches Elektronen-Synchrotron DESY, Hamburg, Germany

V. Drugakov, W. Lohmann, S. Schlenstedt
Deutsches Elektronen-Synchrotron DESY, Zeuthen, Germany

G. Barbagli, E. Gallo
INFN Florence, Florence, Italy [e]

P. G. Pelfer
University and INFN Florence, Florence, Italy [e]

A. Bamberger, D. Dobur, F. Karstens, N.N. Vlasov[18]
Fakultät für Physik der Universität Freiburg i.Br., Freiburg i.Br., Germany [b]

P.J. Bussey[19], A.T. Doyle, W. Dunne, M. Forrest, M. Rosin, D.H. Saxon, I.O. Skillicorn
Department of Physics and Astronomy, University of Glasgow, Glasgow, United Kingdom [m]

I. Gialas[20], K. Papageorgiu
Department of Engineering in Management and Finance, Univ. of Aegean, Greece

U. Holm, R. Klanner, E. Lohrmann, H. Perrey, P. Schleper, T. Schörner-Sadenius, J. Sztuk, H. Stadie, M. Turcato
Hamburg University, Institute of Exp. Physics, Hamburg, Germany [b]

C. Foudas, C. Fry, K.R. Long, A.D. Tapper
Imperial College London, High Energy Nuclear Physics Group, London, United Kingdom [m]

T. Matsumoto, K. Nagano, K. Tokushuku[21], S. Yamada, Y. Yamazaki[22]
Institute of Particle and Nuclear Studies, KEK, Tsukuba, Japan [f]

A.N. Barakbaev, E.G. Boos, N.S. Pokrovskiy, B.O. Zhautykov
Institute of Physics and Technology of Ministry of Education and Science of Kazakhstan, Almaty, Kazakhstan

V. Aushev[23], O. Bachynska, M. Borodin, I. Kadenko, A. Kozulia, V. Libov, D. Lontkovskyi, I. Makarenko, Iu. Sorokin, A. Verbytskyi, O. Volynets
Institute for Nuclear Research, National Academy of Sciences, Kiev and Kiev National University, Kiev, Ukraine

D. Son
Kyungpook National University, Center for High Energy Physics, Daegu, South Korea [g]

J. de Favereau, K. Piotrzkowski
Institut de Physique Nucléaire, Université Catholique de Louvain, Louvain-la-Neuve, Belgium [q]

F. Barreiro, C. Glasman, M. Jimenez, L. Labarga, J. del Peso, E. Ron, M. Soares, J. Terrón, C. Uribe-Estrada, M. Zambrana
Departamento de Física Teórica, Universidad Autónoma de Madrid, Madrid, Spain [l]

F. Corriveau, C. Liu, J. Schwartz, R. Walsh, C. Zhou
Department of Physics, McGill University, Montréal, Québec, Canada H3A 2T8 [a]

T. Tsurugai
Meiji Gakuin University, Faculty of General Education, Yokohama, Japan [f]

A. Antonov, B.A. Dolgoshein, D. Gladkov, V. Sosnovtsev, A. Stifutkin, S. Suchkov
Moscow Engineering Physics Institute, Moscow, Russia [j]

R.K. Dementiev, P.F. Ermolov †, L.K. Gladilin, Yu.A. Golubkov, L.A. Khein, I.A. Korzhavina, V.A. Kuzmin, B.B. Levchenko[24], O.Yu. Lukina, A.S. Proskuryakov, L.M. Shcheglova, D.S. Zotkin
Moscow State University, Institute of Nuclear Physics, Moscow, Russia [k]

I. Abt, A. Caldwell, D. Kollar, B. Reisert, W.B. Schmidke
Max-Planck-Institut für Physik, München, Germany

G. Grigorescu, A. Keramidas, E. Koffeman, P. Kooijman, A. Pellegrino, H. Tiecke, M. Vázquez[12], L. Wiggers
NIKHEF and University of Amsterdam, Amsterdam, Netherlands [h]

N. Brümmer, B. Bylsma, L.S. Durkin, A. Lee, T.Y. Ling
Physics Department, Ohio State University, Columbus, Ohio 43210 [n]

P.D. Allfrey, M.A. Bell, A.M. Cooper-Sarkar, R.C.E. Devenish, J. Ferrando, B. Foster, C. Gwenlan[25], K. Horton[26], K. Oliver, A. Robertson, R. Walczak
Department of Physics, University of Oxford, Oxford United Kingdom [m]

A. Bertolin, F. Dal Corso, S. Dusini, A. Longhin, L. Stanco
INFN Padova, Padova, Italy [e]

P. Bellan, R. Brugnera, R. Carlin, A. Garfagnini, S. Limentani
Dipartimento di Fisica dell' Università and INFN, Padova, Italy [e]

B.Y. Oh, A. Raval, J.J. Whitmore[27]
Department of Physics, Pennsylvania State University, University Park, Pennsylvania 16802 [o]

Y. Iga
Polytechnic University, Sagamihara, Japan [f]

G. D'Agostini, G. Marini, A. Nigro
Dipartimento di Fisica, Università 'La Sapienza' and INFN, Rome, Italy [e]

J.E. Cole[28], J.C. Hart
Rutherford Appleton Laboratory, Chilton, Didcot, Oxon, United Kingdom [m]

C. Heusch, H. Sadrozinski, A. Seiden, R. Wichmann[29], D.C. Williams
University of California, Santa Cruz, California 95064, USA [n]

H. Abramowicz[30], R. Ingbir, S. Kananov, A. Levy, A. Stern
Raymond and Beverly Sackler Faculty of Exact Sciences, School of Physics, Tel Aviv University, Tel Aviv, Israel [d]

M. Kuze, J. Maeda
Department of Physics, Tokyo Institute of Technology, Tokyo, Japan [f]

R. Hori, S. Kagawa[31], N. Okazaki, S. Shimizu, T. Tawara
Department of Physics, University of Tokyo, Tokyo, Japan [f]

R. Hamatsu, H. Kaji[32], S. Kitamura[33], O. Ota[34], Y.D. Ri
Tokyo Metropolitan University, Department of Physics, Tokyo, Japan [f]

R. Cirio, M. Costa, M.I. Ferrero, V. Monaco, C. Peroni, R. Sacchi, V. Sola, A. Solano
Università di Torino and INFN, Torino, Italy [e]

N. Cartiglia, S. Maselli, A. Staiano
INFN Torino, Torino, Italy [e]

M. Arneodo, M. Ruspa
Università del Piemonte Orientale, Novara, and INFN, Torino, Italy [e]

S. Fourletov[7], J.F. Martin, T.P. Stewart
Department of Physics, University of Toronto, Toronto, Ontario, Canada M5S 1A7 [a]

S.K. Boutle[20], J.M. Butterworth, T.W. Jones, J.H. Loizides, M. Wing[35]
Physics and Astronomy Department, University College London, London, United Kingdom [m]

B. Brzozowska, J. Ciborowski[36], G. Grzelak, P. Kulinski, P. Łużniak[37], J. Malka[37], R.J. Nowak, J.M. Pawlak, W. Perlanski[37], T. Tymieniecka[38], A.F. Żarnecki
Warsaw University, Institute of Experimental Physics, Warsaw, Poland

M. Adamus, P. Plucinski[39], A. Ukleja
Institute for Nuclear Studies, Warsaw, Poland

Y. Eisenberg, D. Hochman, U. Karshon
Department of Particle Physics, Weizmann Institute, Rehovot, Israel [c]

E. Brownson, D.D. Reeder, A.A. Savin, W.H. Smith, H. Wolfe
Department of Physics, University of Wisconsin, Madison, Wisconsin 53706, USA [n]

S. Bhadra, C.D. Catterall, Y. Cui, G. Hartner, S. Menary, U. Noor, J. Standage, J. Whyte
Department of Physics, York University, Ontario, Canada M3J 1P3 [a]

[1] also affiliated with University College London, United Kingdom
[2] now at University of Salerno, Italy
[3] also working at Max Planck Institute, Munich, Germany
[4] now at Institute of Aviation, Warsaw, Poland
[5] supported by the research grant no. 1 P03B 04529 (2005-2008)
[6] This work was supported in part by the Marie Curie Actions Transfer of Knowledge project COCOS (contract MTKD-CT-2004-517186)
[7] now at University of Bonn, Germany
[8] now at DESY, group FEB, Hamburg, Germany
[9] also at Moscow State University, Russia
[10] now at University of Liverpool, UK
[11] on leave of absence at CERN, Geneva, Switzerland
[12] now at CERN, Geneva, Switzerland
[13] now at Bologna University, Bologna, Italy
[14] also at Institut of Theoretical and Experimental Physics, Moscow, Russia
[15] also at INP, Cracow, Poland
[16] also at FPACS, AGH-UST, Cracow, Poland
[17] partially supported by Warsaw University, Poland
[18] partly supported by Moscow State University, Russia
[19] Royal Society of Edinburgh, Scottish Executive Support Research Fellow
[20] also affiliated with DESY, Germany
[21] also at University of Tokyo, Japan
[22] now at Kobe University, Japan
[23] supported by DESY, Germany
[24] partly supported by Russian Foundation for Basic Research grant no. 05-02-39028-NSFC-a
[25] STFC Advanced Fellow
[26] nee Korcsak-Gorzo
[27] This material was based on work supported by the National Science Foundation, while working at the Foundation.
[28] now at University of Kansas, Lawrence, USA
[29] now at DESY, group MPY, Hamburg, Germany
[30] also at Max Planck Institute, Munich, Germany, Alexander von Humboldt Research Award
[31] now at KEK, Tsukuba, Japan
[32] now at Nagoya University, Japan
[33] member of Department of Radiological Science, Tokyo Metropolitan University, Japan
[34] now at SunMelx Co. Ltd., Tokyo, Japan
[35] also at Hamburg University, Inst. of Exp. Physics, Alexander von Humboldt Research Award and partially supported by DESY, Hamburg, Germany

[36] also at Łódź University, Poland
[37] member of Łódź University, Poland
[38] also at University of Podlasie, Siedlce, Poland
[39] now at Lund Universtiy, Lund, Sweden
† deceased

[a] supported by the Natural Sciences and Engineering Research Council of Canada (NSERC)

[b] supported by the German Federal Ministry for Education and Research (BMBF), under contract numbers 05 HZ6PDA, 05 HZ6GUA, 05 HZ6VFA and 05 HZ4KHA

[c] supported in part by the MINERVA Gesellschaft für Forschung GmbH, the Israel Science Foundation (grant no. 293/02-11.2) and the U.S.-Israel Binational Science Foundation

[d] supported by the Israel Science Foundation

[e] supported by the Italian National Institute for Nuclear Physics (INFN)

[f] supported by the Japanese Ministry of Education, Culture, Sports, Science and Technology (MEXT) and its grants for Scientific Research

[g] supported by the Korean Ministry of Education and Korea Science and Engineering Foundation

[h] supported by the Netherlands Foundation for Research on Matter (FOM)

[i] supported by the Polish State Committee for Scientific Research, project no. DESY/256/2006 - 154/DES/2006/03

[j] partially supported by the German Federal Ministry for Education and Research (BMBF)

[k] supported by RF Presidential grant N 1456.2008.2 for the leading scientific schools and by the Russian Ministry of Education and Science through its grant for Scientific Research on High Energy Physics

[l] supported by the Spanish Ministry of Education and Science through funds provided by CICYT

[m] supported by the Science and Technology Facilities Council, UK

[n] supported by the US Department of Energy

[o] supported by the US National Science Foundation. Any opinion, findings and conclusions or recommendations expressed in this material are those of the authors and do not necessarily reflect the views of the National Science Foundation.

[p] supported by the Polish Ministry of Science and Higher Education as a scientific project (2006-2008)

[q] supported by FNRS and its associated funds (IISN and FRIA) and by an Inter-University Attraction Poles Programme subsidised by the Belgian Federal Science Policy Office

[r] supported by an FRGS grant from the Malaysian government

1 Introduction

This paper presents cross-section measurements for the exclusive production of a real photon in diffractive e^+p[1] interactions, $ep \to e\gamma p$, a process known as deeply virtual Compton scattering (DVCS). In perturbative QCD, this process is described by the exchange of two partons, with different longitudinal and transverse momenta in a colourless configuration. At the $\gamma^* p$ centre-of-mass energies, W, available for ep collisions at the HERA collider, for large momentum-transfer squared at the lepton vertex, Q^2, the DVCS process is dominated by two-gluon exchange. Measurements of the DVCS cross section provide constraints on the generalised parton distributions (GPDs) [1–5], which carry information about the wave function of the proton) [2]. The transverse distribution of partons in the proton, which is not accessible via the F_2 proton structure function, is accounted for in the dependence of the GPDs on the four-momentum transfer squared at the proton vertex, t. The initial and final states of the DVCS process are identical to those of the purely electromagnetic Bethe-Heitler (BH) process. The interference between these two processes in principle provides information about the real and imaginary parts of the QCD scattering amplitude [6–8]. However, the interference is expected to be small in the kinematic region studied in this paper [6, 7].

The simplicity of the final state and the absence of complications due to hadronisation mean that the QCD predictions for DVCS are expected to be more reliable than for exclusive vector meson production which has been extensively studied in ep collisions at HERA [9–16]. Several measurements of DVCS at high W are available [17–20]. The analysis presented here is based on data in the kinematic range of $1.5 < Q^2 < 100\,\mathrm{GeV}^2$ and $40 < W < 170\,\mathrm{GeV}$, an extension compared to the previous ZEUS measurement [18]. A subsample of the data in which the scattered proton is measured in the ZEUS leading proton spectrometer (LPS) [21] is used for the direct measurement of the t dependence of the DVCS cross section.

2 Experimental set-up

The data used for this measurement were taken with the ZEUS detector at the HERA ep collider in the years 1999 and 2000, when HERA collided positrons of energy 27.5 GeV with protons of energy 920 GeV, and correspond to an integrated luminosity of 61.1 pb^{-1}. The subsample used to measure the t distribution was collected in 2000 and corresponds to an integrated luminosity of 31.3 pb^{-1}.

[1] Hereafter, the positron is referred to with the same symbol, e, as the electron.

A detailed description of the ZEUS detector can be found elsewhere [23, 24]. A brief outline of the components most relevant for this analysis is given below.

Charged particles were tracked in the CTD [25]. The CTD operated in a magnetic field of 1.43 T provided by a thin solenoid. It consisted of 72 cylindrical drift-chamber layers, organised in nine superlayers covering the polar-angle [2] region $15^\circ < \theta < 164^\circ$. The transverse-momentum resolution for full-length tracks was $\sigma(p_T)/p_T = 0.0058 p_T \oplus 0.0065 \oplus 0.0014/p_T$, with p_T in GeV.

The uranium–scintillator calorimeter (CAL) [26] covered 99.7% of the total solid angle and consisted of three parts: the forward (FCAL), the barrel (BCAL) and the rear (RCAL) calorimeters. Each part was subdivided transversely into towers and longitudinally into one electromagnetic section (EMC) and either one (in RCAL) or two (in BCAL and FCAL) hadronic sections (HAC). The CAL energy resolutions, as measured under test-beam conditions, were $\sigma(E)/E = 0.18/\sqrt{E}$ for positrons and $\sigma(E)/E = 0.35/\sqrt{E}$ for hadrons, with E in GeV.

The position of positrons scattered at small angles to the positron-beam direction was determined combining the information from the CAL, the small-angle rear tracking detector (SRTD) and the hadron-electron separator (HES) [27, 28].

The FPC [29] was used to measure the energy of particles in the pseudorapidity range $\eta \approx 4.0 - 5.0$. It consisted of a lead–scintillator sandwich calorimeter installed in the 20×20 cm^2 beam hole of the FCAL. The energy resolution for electrons as measured in a test beam, was $\sigma(E)/E = (0.41 \pm 0.02)/\sqrt{E} \oplus 0.062 \pm 0.002$, with E in GeV. The energy resolution for pions was $\sigma(E)/E = (0.65 \pm 0.02)/\sqrt{E} \oplus 0.06 \pm 0.01$, with E in GeV, after having combined the information from FPC and FCAL. The e/h ratio was close to unity.

The LPS [21] detected positively charged particles scattered at small angles and carrying a substantial fraction, x_L, of the incoming proton momentum; these particles remained in the beam-pipe and their trajectory was measured by a system of silicon microstrip detectors that was inserted very close (typically within a distance of a few mm) to the proton beam. The detectors were grouped in six stations, S1 to S6, placed along the beam-line in the direction of the proton beam, between 23.8 m and 90.0 m from the interaction point. The particle deflections induced by the magnets of the proton beam-line allowed a momentum analysis of the scattered proton. For the present measurements, only stations S4, S5 and S6 were used. The resolutions were about 0.5% on the longitudinal momentum fraction and about 5 MeV on the transverse momentum. The LPS acceptance [22] was

[2] The ZEUS coordinate system is a right-handed Cartesian system, with the Z axis pointing in the proton direction, referred to as the "forward direction", and the X axis pointing left towards the centre of HERA. The coordinate origin is at the nominal interaction point. The pseudorapidity is defined as $\eta = -\ln(\tan\frac{\theta}{2})$, where the polar angle θ is measured with respect to the proton beam direction.

approximately 2% and x_L-independent for $x_L \gtrsim 0.98$; it increased smoothly to about 10% as x_L decreased to 0.9.

The luminosity was measured from the rate of the bremsstrahlung process $ep \to e\gamma p$, where the photon was measured in a lead–scintillator calorimeter [30] placed in the HERA tunnel at $Z = -107$ m.

3 Monte Carlo simulations

The acceptance and the detector response were determined using Monte Carlo (MC) simulations. The detector was simulated in detail using a program based on GEANT 3.13 [31]. All of the simulated events were processed through the same reconstruction and analysis chain as the data.

A MC generator, GENDVCS [32], based on a model by Frankfurt, Freund and Strikman (FFS) [33], was used to simulate the elastic DVCS process as described in [18]. The ALLM97 [34] parameterisation of the F_2 proton structure function of the proton was used as input. The t dependence was assumed to be exponential with a slope parameter b set to 4.5 GeV^{-2}, independent of W and Q^2.

The elastic, $ep \to e\gamma p$, and quasi-elastic $ep \to e\gamma Y$ BH processes, where Y is a low-mass state, and the exclusive dilepton production, $ep \to ee^+e^-p$, were simulated using the GRAPE-COMPTON[3] [35] and the GRAPE-DILEPTON [35] generators. These two MC programs are based on the automatic system GRACE [36] for calculating Feynman diagrams. A possible contribution from vector meson electroproduction was simulated with the ZEUSVM generator [37]. To account for electroweak radiative effects, all the generators were interfaced to HERACLES 4.6 [38].

4 Kinematic variables and event selection

The process $ep \to e\gamma p$ is parametrised by the following variables:

- $Q^2 = -q^2 = -(k - k')^2$, the negative four-momentum squared of the virtual photon, where k (k') is the four-momentum of the incident (scattered) positron;
- $W^2 = (q + p)^2$, the squared centre-of-mass energy of the photon-proton system, where p is the four-momentum of the incident proton;

[3] Hereafter, the GRAPE-COMPTON generator is referred to as GRAPE.

- $x = Q^2/(2P \cdot q)$, the fraction of the proton momentum carried by the quark struck by the virtual photon in the infinite-momentum frame (the Bjorken variable);
- $x_L = \frac{p' \cdot k}{p \cdot k}$, the fractional momentum of the outgoing proton, where p' is the four-momentum of the scattered proton;
- $t = (p - p')^2$, the squared four-momentum transfer at the proton vertex.

For the Q^2 range of this analysis, $Q^2 > 1.5$ GeV^2, and at small values of t, the signature of elastic DVCS and BH events consists of a scattered positron, a photon and a scattered proton. The scattered proton remains in the beam-pipe where, for a subsample of events, it is detected in the LPS (LPS sample).

The events were selected online via a three-level trigger system [23, 39]. The trigger required events with two isolated electromagnetic (EM) clusters with energy greater than 2 GeV. The trigger efficiency was studied as a function of the lowest energy cluster, it was found to increase from 80% to 100% for increasing cluster energy and the Monte Carlo was reweighed according.

The offline selection followed the strategy described in [18]. Two EM clusters were found by a dedicated, neural-network based, positron finder [40]. They were ordered in polar-angle and are in the following denoted as EM1 and EM2, with $\theta_1 > \theta_2$. The first cluster was required to be in the RCAL with energy $E_1 > 10\,\text{GeV}$; the second cluster had to have a polar angle $\theta_2 < 2.85\,\text{rad}$ and was required to be either in the RCAL, with energy $E_2 > 3\,\text{GeV}$, or in the BCAL, with energy $E_2 > 2.5\,\text{GeV}$. The angular range of the second cluster corresponds to the region of high reconstruction efficiency for tracks in the CTD. The association of a track discriminates between positron and photon induced clusters. For events with one track, a match was required between the track and one of the two EM clusters. Events with more than one track were rejected. To ensure full containement of the electromagnetic shower, the impact position of each EM cluster on the face of RCAL was required to be outside a rectangular area of 26×16 cm^2 around the beam-pipe.

The condition $40 < E - P_Z < 70$ GeV was imposed, with $E = E_1 + E_2$ and $P_Z = E_1 \cos\theta_1 + E_2 \cos\theta_2$. This requirement rejected photoproduction events and also events in which a hard photon was radiated from the incoming positron.

Events with CAL energy deposits not associated with the two EM clusters were rejected if their energy was above the noise level in the CAL [41]. In addition, the total energies measured in the FPC and in the FCAL were each required to be below 1 GeV [10, 41]. These elasticity requirements also suppressed DVCS events and inelastic BH events in which the proton dissociates into a high-mass hadronic system. The sample was still contaminated by events in which a forward, low-mass hadronic system was not visible in the main detector. Alternatively, a clean sample of elastic DVCS and BH events was obtained by additionally requiring the proton to be detected in the LPS.

The LPS event was rejected if, at any point, the distance of the proton track candidate to the beam-pipe was less than 0.04 cm. It was also rejected if the X position of the track impact point at station S4 was smaller than -3.3 cm. These cuts reduced the sensitivity of the acceptance on the uncertainty in the position of the beam-pipe apertures. To suppress background from overlays of ep collisions with protons originating from the beam-halo, it was required that $(E + P_Z) + 2p_Z^{\rm LPS} < 1865$ GeV, where $p_Z^{\rm LPS}$ is the longitudinal momentum of the scattered proton. The variable x_L was required to be within the range $0.96 < x_L < 1.02$ to exclude non-elastic events [42, 43]. The variable t was required to be in the range $0.08 < |t| < 0.53$ GeV^2 where the LPS acceptance was high and slowly changing.

The kinematic region was $40 < W < 170$ GeV and $1.5 < Q^2 < 100$ GeV^2. For the purposes of this analysis, the values of Q^2 and W were determined for each event, independently of its topology, under the assumption that the EM1 cluster is the scattered positron. This assumption is always valid for DVCS events for the Q^2 range considered here. The electron method [44] was used to determine Q^2 and the double-angle method [44] to determine W.

5 Background study and signal extraction

The selected events were subdivided into three samples,

- γ sample: EM2, with no track pointing to it, is taken to be the photon and EM1 is assumed to be the scattered positron. Both BH and DVCS processes contribute to this topology. The sample consisted of 7618 events and 55 events after the LPS selection.
- e sample: EM2, with a positive-charge track pointing to it, is assumed to be the scattered positron and EM1 is the photon. The sample is dominated by BH events. The number of DVCS events is predicted to be negligible due to the large Q^2 implied by the large positron scattering angle. This sample consisted of 11988 events and 33 events after the LPS selection.
- negative-charge-e sample: EM2, with a negative-charge track pointing to it, may have originated from an e^+e^- final state accompanying the scattered positron, where one of the positrons escaped detection. This sample is dominated by non-resonant e^+e^- production and by J/ψ production with subsequent decay into e^+e^- and was used to study these background sources. It consisted of 764 events and only one event after the LPS selection.The diffractive electroproduction of ρ, ω and ϕ mesons was found to be negligible [18].

In the kinematic region of this analysis, the contribution of the interference term between the DVCS and BH amplitudes is very small when the cross section is integrated over the

angle between the positron and proton scattering planes [6, 7]. Thus the cross section for exclusive production of real photons was treated as a simple sum over the contributions from the DVCS and BH processes. The DVCS cross section was determined by subtracting the latter.

The size of the BH contribution to be subtracted was determined using the e sample which consists of elastic and inelastic BH events and a small fraction of exclusive e^+e^- production. The exclusive e^+e^- contribution was estimated with the negative-charge-e sample to be $(6.4 \pm 0.2)\%$ and subtracted from the e sample.

The inelastic fraction of the BH events was estimated from the difference in the azimuthal angles, $\Delta\phi$, between the two electromagnetic clusters in the e sample. It was determined to be $(16 \pm 1)\%$ and was negligible in the LPS tagged subsample [45].

The measured cross section of the BH process was $(4 \pm 1)\%$ smaller than the expectations of the GRAPE program (a detailed discussion can be found elsewhere [45,46]). The GRAPE cross section was modified accordingly.

The BH contribution to the γ sample was determined by GRAPE and found to be $(56 \pm 1)\%$ for the untagged and $(21 \pm 3)\%$ for the LPS tagged sample. The BH-subtracted γ sample was further scaled by $(1 - f_{p-\mathrm{diss}})$, where $f_{p-\mathrm{diss}}$ is the fraction of DVCS events in which the proton dissociated into a low-mass state. Its value was taken, as in [18], from previous publication [47], $f_{p-\mathrm{diss}} = 17.5 \pm 1.3^{+3.7}_{-3.2}\%$.

The W and Q^2 distributions in the untagged sample (inclusive sample) and the x_L and t distributions in the LPS sample, separately for the e sample, for the γ sample and for the γ sample after BH and proton dissociation background subtraction, are shown in Fig. 1. Also shown in the figure are MC expectations which describe the data well.

6 Systematic uncertainties

The uncertainties due to the reconstruction of the scattered positron and to the background subtraction were evaluated by varying the selection criteria as follows:

- varying the electromagnetic energy scale by $\pm 2\%$;
- restricting the $E - P_Z$ cut to $45 < E - P_Z < 65$ GeV;
- shifting the reconstructed position of the positron with respect to the MC by $\pm$1mm;
- changing the elasticity requirements by ± 30 MeV in the EMC and ± 50 MeV in the HAC sections;
- changing the photon candidate energy by $\pm 10\%$;

- varying the inelastic BH fraction by $\pm 1\%$.

Each individual systematic uncertainty affects single bins in Q^2 and W typically by less than 5% and by less than 10% in all cases bar the highest Q^2 bin where statistical fluctuations dominate.

To evaluate the uncertainties due to the reconstruction of the final-state proton,

- the cut on the minimum distance to the beam-pipe was increased to 0.1 cm;
- the t range was tightened to $0.1 < |t| < 0.5$ GeV^2;
- the kinematic limit of the beam-halo background cut was lowered to 1855 GeV;
- the x position of the track impact point at station S4 was restricted to -32 mm.

The total systematic uncertainty was obtained by adding in quadrature the individual contributions. It was found to be $\pm 8\%$ on average which is smaller than the statistical uncertainties.

For the inclusive sample the uncertainty in the determination of the integrated luminosity of $\pm 2.25\%$ and on the proton-dissociative background of $^{+3.9}_{-3.5}\%$ are not included in the figures and in the tables.

For the LPS data, there is an overall uncertainty of $\pm 7\%$ which originates mostly from the uncertainty on the simulation of the proton-beam optics. It can be treated as a normalisation uncertainty as it is largely independent of the kinematic variables and is not included in the figures and in the tables. It also includes the uncertainty on the integrated luminosity for the LPS sample of $\pm 2.25\%$.

7 Cross section determination and results

The $\gamma^* p$ cross section of the DVCS process was evaluated as a function of W, Q^2 using the expression

$$\sigma^{\gamma^* p \to \gamma p}(W_i, Q_i^2) = \frac{(N_i^{\rm obs} - N_i^{\rm BH}) \cdot (1 - f_{p-{\rm diss}})}{N_i^{\rm MC}} \cdot \sigma^{{\rm FFS}(\gamma^* p \to \gamma p)}(W_i, Q_i^2),$$

where $N_i^{\rm obs}$ is the total number of data events in the γ sample in bin i of W and Q^2, $N_i^{\rm BH}$ denotes the number of elastic and inelastic BH events in the γ sample in the bin, and $N_i^{\rm MC}$ is the number of events expected in the γ sample from GenDVCS for the luminosity of the data. The cross section as predicted by the FFS model is denoted $\sigma^{\rm FFS}(\gamma^* p \to \gamma p)$ and was evaluated at the centre (W_i, Q_i^2) of each Q^2 and W bin. The differential cross section as a function of t was calculated from the LPS tagged sample for which $f_{p-{\rm diss}}$ is zero. All the results are listed in Tables 1 – 4.

The $\gamma^* p$ DVCS cross section, $\sigma^{\gamma^* p \to \gamma p}$, is presented in Fig. 2 as a function of Q^2 at $W = 104$ GeV and as a function of W at $Q^2 = 3.2$ GeV^2. The cross section shows a fast decrease with Q^2. A fit to the Q^2 dependence of the cross section, assuming the functional form $\sigma^{\gamma^* p \to \gamma p}(Q^2) \sim Q^{-2n}$, was performed for $W = 104$ GeV yielding $n = 1.54 \pm 0.05$(stat.), smaller than expected for a pure propagator term [33]. The result is in agreement with other DVCS measurements at HERA at lower W [17–20]. As expected for DVCS [33], the decrease of the cross section with Q^2 is slower than for exclusive vector meson production [12–16, 48]. The cross section increases with W. In pQCD-based models, this behaviour is related to the increase of the gluon content of the proton with decreasing Bjorken-x. A fit to the W dependence of the cross section, assuming a functional form $\sigma^{\gamma^* p \to \gamma p}(W) \sim W^{\delta}$, was performed for $Q^2 = 3.2$ GeV^2, yielding $\delta = 0.52 \pm 0.09$(stat.). This result is in agreement with the previous measurements [17–20] performed in a restricted range of W and at higher Q^2. A second fit restricted to the region $1.5 < Q^2 < 5$ GeV^2 at $Q^2 = 2.4$ GeV^2, was also performed giving $\delta = 0.44 \pm 0.19$(stat.). The fit is presented in Fig. 3. Also shown in the figure are previous ZEUS measurements at different values of Q^2 [18] and the extension to higher W values from the present analysis. For each Q^2 the corresponding δ values fitted in the extended W range are given. Within the present accuracy the results do not show evidence for a Q^2 dependence of δ. This result is similar to that obtained for the exclusive production of J/ψ mesons [12–14, 47].

The first direct measurement of the differential cross section $d\sigma^{\gamma^* p \to \gamma p}/dt$, extracted from the LPS-tagged events at $Q^2 = 3.2$ GeV^2 and at $W = 104$ GeV, is shown in Fig. 4. The value of the slope parameter b extracted from an exponential fit to the differential cross section, $d\sigma^{\gamma^* p \to \gamma p}/dt \propto e^{-b|t|}$, is $b = 4.5 \pm 1.3$(stat.) ± 0.4(syst.) GeV^{-2} (χ^2/ndf $= 0.90$). This value is consistent with the results obtained by H1 [20] $b = 5.45 \pm 0.19$(stat.) $\pm$ 0.34(syst.) GeV^{-2} at $Q^2 = 8$ GeV^2 and $W = 82$ GeV, from the transverse-momentum distribution of the photon candidate.

A compilation of b values as measured for various exclusive processes [14, 21], including the result of this paper, is shown in Fig. 5 as a function of $Q^2 + M^2$, where M is the mass of the exclusive final state. The b value presented here is lower but consistent with the corresponding vector mesons and H1 DVCS values at similar scales. The fast rise of the DVCS cross section with W at $Q^2 = 2.4$ GeV^2 and the low value of b at $Q^2 = 3.2$ GeV^2 indicate that the DVCS process is a hard process even at low Q^2 values.

8 Summary

The DVCS cross section has been measured as a function of Q^2 and W in the region $1.5 < Q^2 < 100$ GeV^2 and $40 < W < 170$ GeV. The measured cross section decreases

steeply with Q^2, showing a dependence Q^{-2n}, with $n = 1.54 \pm 0.05$(stat.). The W cross section rises with increasing W following a functional form W^{δ}, with $\delta = 0.52 \pm 0.09$(stat.) and has little dependence on Q^2.

For the first time, the DVCS differential cross section as a function of t was measured by directly tagging the scattered proton. An exponential behaviour was assumed, the slope parameter $b = 4.5 \pm 1.3$(stat.) ± 0.4(syst.) GeV^{-2} was obtained from a fit to the data at $Q^2 = 3.2$ GeV^2 and $W = 104$ GeV. These findings indicate that the DVCS process is a hard process even at low Q^2.

Acknowledgements

We thank the DESY Directorate for their support and encouragement. We are grateful for the support of the DESY computing and network services. We are specially grateful to the HERA machine group: collaboration with them was crucial to the successful installation and operation of the leading proton spectrometer. The design, construction and installation of the ZEUS detector were made possible by the ingenuity and effort of many people who are not listed as authors.

References

[1] M. Diehl, T. Gousset, B. Pire and J. Ralston, Phys. Lett. **B 411**, 193 (1997).

[2] M. Burkardt, Int. J. Mod. Phys. **A 18**, 173 (2003).

[3] M. Diehl, Eur. Phys. J. **C 25**, 223 (2002).

[4] V. Guzey and T. Teckentrup, Phys. Rev. **D 74**, 54027 (2006).

[5] K. Kumericki, D. Mueller and K. Passek-Kumericki, Nucl. Phys. **B 794**, 244 (2008).

[6] L. Frankfurt, A. Freund and M. Strikman, Phys. Lett. **B 460**, 417 (1999).

[7] A.V. Belitsky, D. Müller and A. Kirchner, Nucl. Phys. **B 629**, 323 (2002).

[8] A. Freund and M. McDermott, Phys. Rev. **D 65**, 091901 (2002).

[9] ZEUS Coll., J. Breitweg et al., Phys. Lett. **B 487**, 273 (2000).

[10] ZEUS Coll., S. Chekanov et al., Nucl. Phys. **B 718**, 2 (2005).

[11] ZEUS Coll., S. Chekanov et al., Nucl. Phys. **B 695**, 3 (2004).

[12] ZEUS Coll., J. Breitweg et al., Eur. Phys. J. **C 14**, 213 (2000).

[13] H1 Coll., C. Adloff et al., Phys. Lett. **B 483**, 360 (2000).

[14] ZEUS Coll., S. Chekanov et al., PMC Phys. **A 1**, 6 (2007).

[15] H1 Coll., A. Aktas et al., Eur. Phys. J. **C 46**, 585 (2006).

[16] H1 Coll., C. Adloff et al., Eur. Phys. J. **C 13**, 371 (2000).

[17] H1 Coll., C. Adloff et al., Phys. Lett. **B 517**, 47 (2001).

[18] ZEUS Coll., S. Chekanov et al., Phys. Lett. **B 573**, 46 (2003).

[19] H1 Coll., A. Aktas et al., Eur. Phys. J. **C 44**, 1 (2005).

[20] H1 Coll., F.D. Aktas et al., Phys. Lett. **B 659**, 796 (2008).

[21] ZEUS Coll., M. Derrick et al., Z. Phys. **C 73**, 253 (1997).

[22] ZEUS Coll., S. Chekanov et al., Eur. Phys. J. **C 38**, 43 (2004).

[23] ZEUS Coll., U. Holm (ed.), *The ZEUS Detector*. Status Report (unpublished), DESY (1993), available on `http://www-zeus.desy.de/bluebook/bluebook.html`.

[24] ZEUS Coll., M. Derrick et al., Phys. Lett. **B 293**, 465 (1992).

[25] N. Harnew et al., Nucl. Inst. Meth. **A 279**, 290 (1989);
B. Foster et al., Nucl. Phys. Proc. Suppl. **B 32**, 181 (1993);
B. Foster et al., Nucl. Inst. Meth. **A 338**, 254 (1994).

[26] M. Derrick et al., Nucl. Inst. Meth. **A 309**, 77 (1991);
A. Andresen et al., Nucl. Inst. Meth. **A 309**, 101 (1991);
A. Caldwell et al., Nucl. Inst. Meth. **A 321**, 356 (1992);
A. Bernstein et al., Nucl. Inst. Meth. **A 336**, 23 (1993).

[27] A. Bamberger et al., Nucl. Inst. Meth. **A 401**, 63 (1997).

[28] A. Dwurazny et al., Nucl. Inst. Meth. **A 277**, 176 (1989).

[29] ZEUS Coll., FPC group, A. Bamberger et al., Nucl. Inst. Meth. **A 450**, 235 (2000).

[30] J. Andruszków et al., Preprint DESY-92-066, DESY, 1992;
ZEUS Coll., M. Derrick et al., Z. Phys. **C 63**, 391 (1994);
J. Andruszków et al., Acta Phys. Pol. **B 32**, 2025 (2001).

[31] R. Brun et al., *GEANT3.* Technical Report CERN-DD/EE/84-1,CERN, 1987.

[32] P.R.B. Saull, *A Monte Carlo Generator for Deeply Virtual Compton Scattering at HERA*, 1999, available on `http://www-zeus.desy.de/physics/diff/pub/MC`.

[33] L.L. Frankfurt, A. Freund and M. Strikman, Phys. Rev. **D 58**, 114001 (1998). Erratum-ibid **D 59** (1999) 119901.

[34] H. Abramowicz and A. Levy, Preprint DESY-97-251 (hep-ph/9712415), DESY, 1997.

[35] T. Abe, Comp. Phys. Comm. **136**, 126 (2001).

[36] T. Ishikawa et al., *GRACE manual: Automatic generation of tree amplitudes in Standard Models: Version 1.0.* KEK Report 92-19, 1993.

[37] K. Muchorowski, Ph.D. Thesis, Warsaw University, 1998 (unpublished).

[38] H. Spiesberger, *An Event Generator for ep Interactions at HERA Including Radiative Processes (Version 4.6)*, 1996, available on `http://www.desy.de/~hspiesb/heracles.html`.

[39] W.H. Smith, K. Tokushuku and L.W. Wiggers, *Proc. Computing in High-Energy Physics (CHEP),* Annecy, France, Sept. 1992, C. Verkerk and W. Wojcik (eds.), p. 222, CERN, Geneva, Switzerland (1992). Also in preprint DESY 92-150B.

[40] H. Abramowicz, A. Caldwell and R. Sinkus, Nucl. Inst. Meth. **A 365**, 508 (1995);
R. Sinkus and T. Voss, Nucl. Inst. Meth. **A 391**, 360 (1997).

[41] R. Ciesielski, *Exclusive J/Psi Production in Deep Inelastic ep Scattering in the ZEUS exeriment at HERA.* Ph.D. Thesis, Warsaw University, Warsaw, Poland, 2004.

[42] ZEUS Coll., S. Chekanov et al., Preprint DESY-08-176, DESY, 2008.

[43] ZEUS Coll., S. Chekanov et al., PMC Phys. **A 1**, 6 (2007).

[44] S. Bentvelsen, J. Engelen and P. Kooijman, *Proc. Workshop on Physics at HERA*, W. Buchmüller and G. Ingelman (eds.), Vol. 1, p. 23, Hamburg, Germany, DESY (1992);
K.C. Höger, ibid, p.43.

[45] S. Fazio, *Measurement of Deeply Virtual Compton Scattering cross sections at HERA and a new model for the DVCS amplitude.* Ph.D. Thesis, Calabria University, Rende (Cosenza), Italy, 2007, available on `http://www-zeus.desy.de/physics/diff/pub/theses.html`.

[46] I. Grabowska-Bołd, *Measurement of Deeply Virtual Compton Scattering Using the ZEUS Detector at HERA.* Ph.D. Thesis, University of Mining and Metallurgy, Cracow, Poland, Report DESY-THESIS-2004-034, 2003.

[47] ZEUS Coll., S. Chekanov et al., Eur. Phys. J. **C 24**, 345 (2002).

[48] ZEUS Coll., J. Breitweg et al., Eur. Phys. J. **C 6**, 603 (1999).

$\sigma^{\gamma^* p \to \gamma p}$		
Q^2 range (GeV^2)	Q^2 (GeV^2)	$\sigma^{\gamma^* p \to \gamma p}$ (nb)
1.5 - 5	3.25	$21.28 \pm 0.92^{+1.02}_{-1.34}$
5 - 10	7.5	$5.87 \pm 0.42^{+0.14}_{-0.30}$
10 - 15	12.5	$3.27 \pm 0.33^{+0.07}_{-0.16}$
15 - 25	20.0	$1.23 \pm 0.21^{+0.05}_{-0.08}$
25 - 40	32.5	$0.55 \pm 0.18^{+0.04}_{-0.04}$
40 - 100	70.0	$0.16 \pm 0.07^{+0.02}_{-0.02}$

Table 1: *The DVCS cross section, $\sigma^{\gamma^* p \to \gamma p}$, as a function of Q^2. Values are quoted at the centre of each Q^2 bin and at $W = 104\,GeV$. The first uncertainty is statistical and the second systematic.*

$\sigma^{\gamma^* p \to \gamma p}$		
W range (GeV)	W (GeV)	$\sigma^{\gamma^* p \to \gamma p}$ (nb)
40 - 60	50	$14.47 \pm 1.05^{+0.50}_{-0.88}$
60 - 80	70	$20.38 \pm 1.57^{+1.01}_{-1.99}$
80 - 100	90	$17.95 \pm 1.35^{+0.64}_{-0.93}$
100 - 120	110	$20.65 \pm 1.26^{+0.59}_{-1.16}$
120 - 140	130	$26.42 \pm 1.84^{+0.79}_{-0.88}$
140 - 170	155	$27.60 \pm 3.74^{+2.01}_{-3.34}$

Table 2: *The DVCS cross section, $\sigma^{\gamma^* p \to \gamma p}$, as a function of W. Values are quoted at the centre of each W bin and for $Q^2 = 3.2\,GeV^2$. The first uncertainty is statistical and the second systematic.*

$\sigma^{\gamma^* p \to \gamma p}$					
W range (GeV)	W (GeV)	$\sigma^{\gamma^* p \to \gamma p}$ (nb) $Q^2 = 2.4$ GeV^2	$\sigma^{\gamma^* p \to \gamma p}$ (nb) $Q^2 = 6.2$ GeV^2	$\sigma^{\gamma^* p \to \gamma p}$ (nb) $Q^2 = 9.9$ GeV^2	$\sigma^{\gamma^* p \to \gamma p}$ (nb) $Q^2 = 18.0$ GeV^2
40 - 65	52.5	$27.06 \pm 3.44^{+4.37}_{-4.42}$			
65 - 90	77.5	$22.36 \pm 3.11^{+3.40}_{-1.73}$			
90 - 115	102.5	$26.49 \pm 1.89^{+0.89}_{-1.44}$			
115 - 140	127.5	$35.94 \pm 2.63^{+1.81}_{-1.89}$			
140 - 170	155	$35.72 \pm 9.47^{+3.01}_{-2.94}$	$16.93 \pm 2.43^{+1.37}_{-1.40}$	$6.15 \pm 1.67^{+0.51}_{-0.51}$	$2.21 \pm 0.82^{+0.18}_{-0.18}$

Table 3: *The DVCS cross section, $\sigma^{\gamma^* p \to \gamma p}$, as a function of W in four Q^2 ranges. Values are quoted at the centre of each W bin and for the Q^2 values listed. The first uncertainty is statistical and the second systematic. The values for higher Q^2 and lower W, shown in Fig. 3, are taken from a previous publication [18] and are not repeated here.*

$d\sigma^{\gamma^* p \to \gamma p}/dt$		
t range (GeV^2)	t (GeV^2)	$\sigma^{\gamma^* p \to \gamma p}/dt$ (nb/GeV^2)
0.08 - 0.19	0.14	$34.6 \pm 9.6 \pm 2.4$
0.19 - 0.31	0.25	$32.7 \pm 9.4 \pm 2.3$
0.31 - 0.42	0.36	$19.6 \pm 7.5 \pm 1.4$
0.42 - 0.53	0.47	$5.7 \pm 4.1 \pm 0.4$

Table 4: *The DVCS differential cross section, $d\sigma^{\gamma^* p \to \gamma p}/dt$, as a function of $|t|$. Values are quoted at the centre of each $|t|$ bin and for $Q^2 = 3.2\,GeV^2$ and $W = 104\,GeV$. The first uncertainty is statistical and the second systematic.*

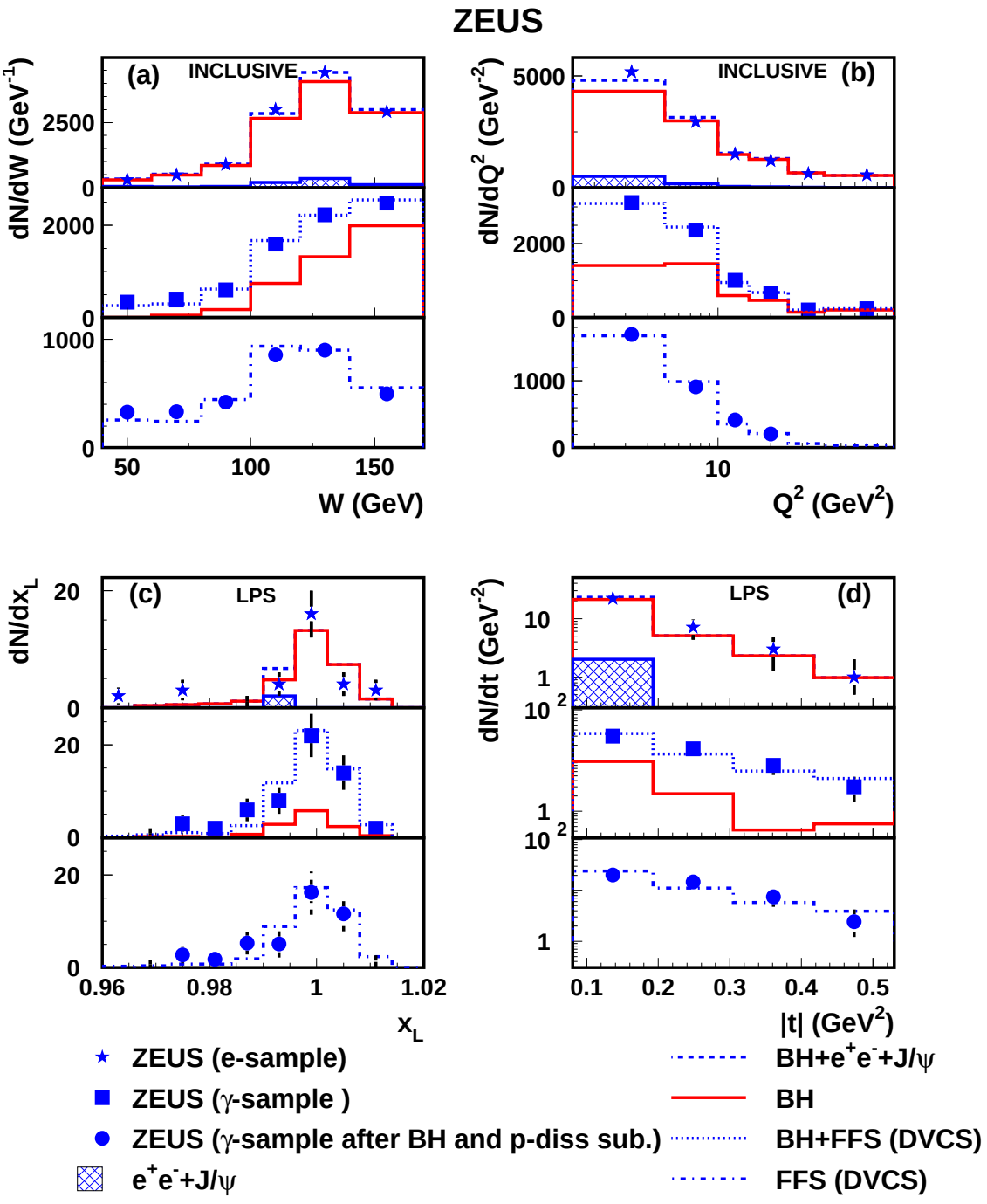

Figure 1: *Distribution of (a) W, (b) Q^2 in the inclusive sample and of (c) x_L and (d) $|t|$ in the LPS sample, for the e-sample (top), the γ-sample (middle) and the γ-sample after BH background and proton dissociation subtraction (bottom). Also shown are the expectations of the MC normalised to the luminosity of the data and the contribution from exclusive dilepton production (e^+e^-).*

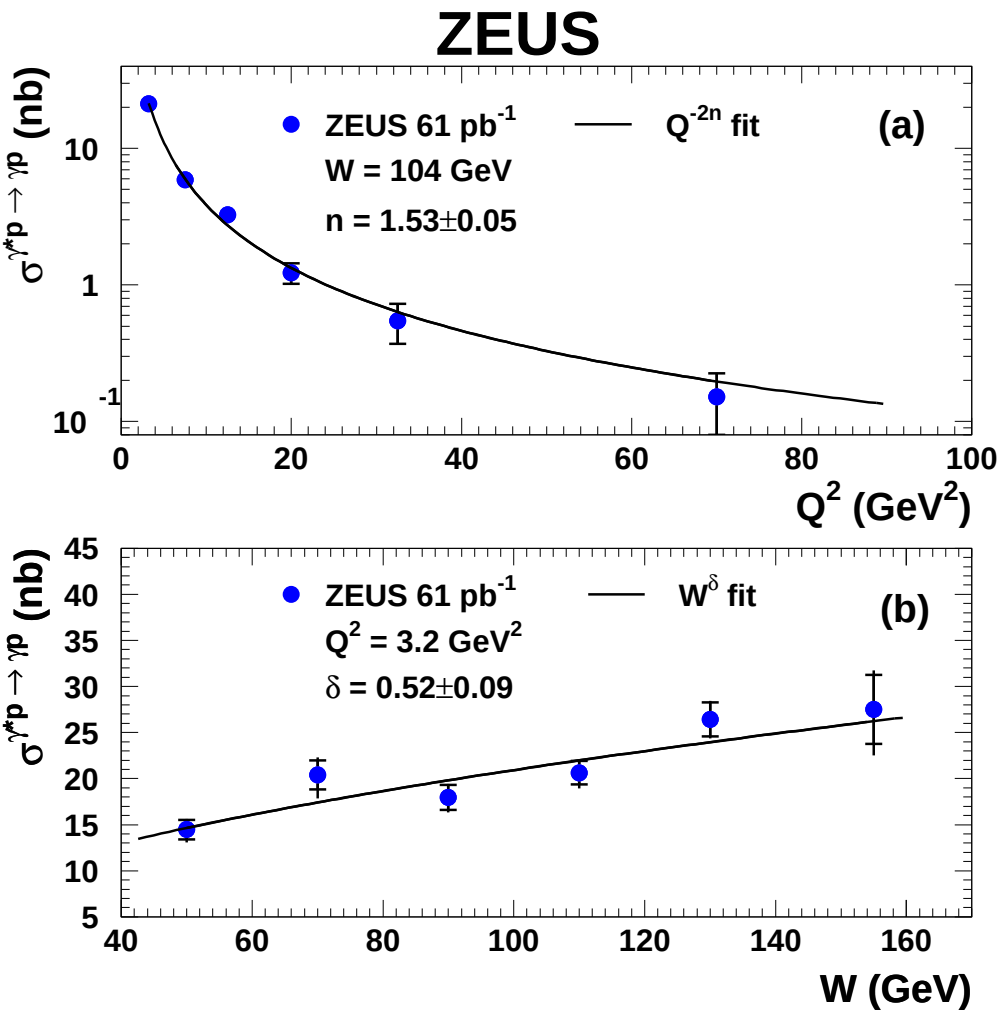

Figure 2: *(a) The DVCS cross section, $\sigma^{\gamma^* p \to \gamma p}$, as a function of Q^2. The solid line is the result of a fit of the form $\sim Q^{-2n}$. (b) The DVCS cross section, $\sigma^{\gamma^* p \to \gamma p}$, as a function of W. The solid line is the result of a fit of the form $\sim W^{\delta}$. The inner error bars represent the statistical uncertainty while the outer error bars the statistical and systematic uncertainties added in quadrature.*

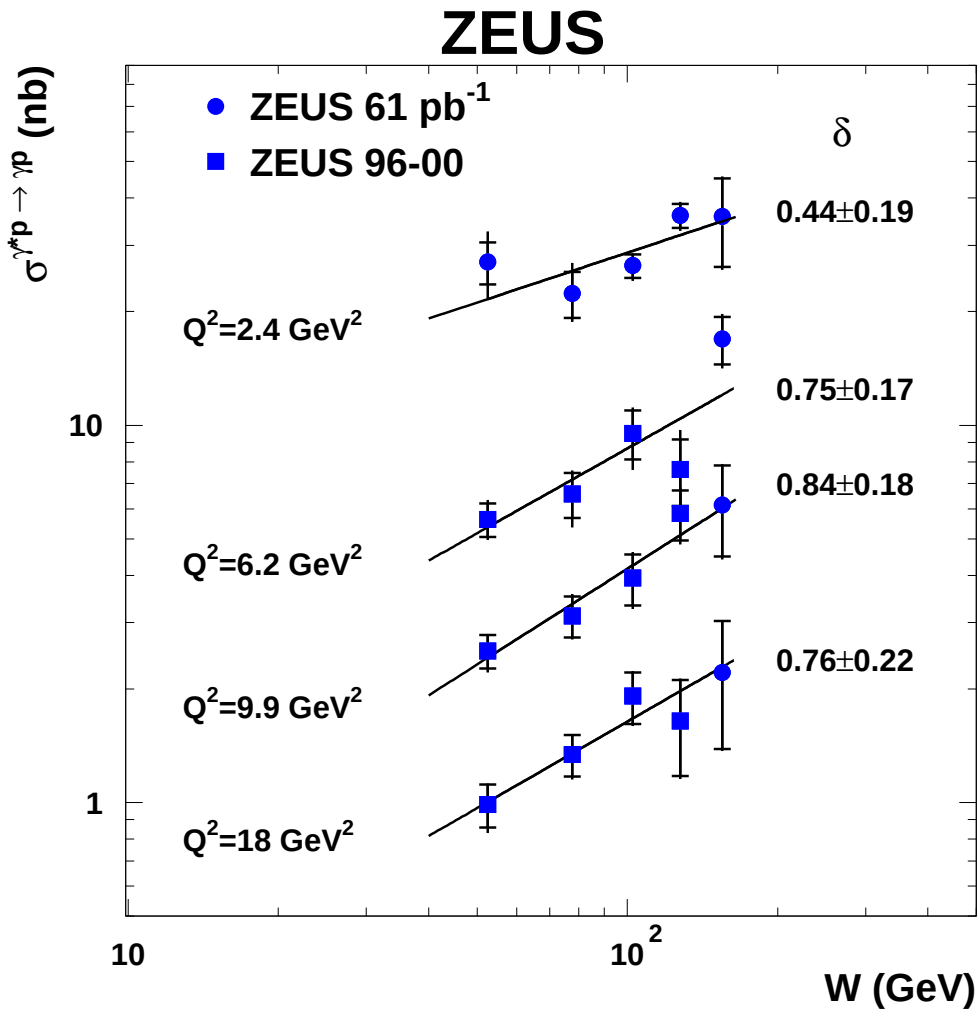

Figure 3: *The DVCS cross section, $\sigma^{\gamma^* p \to \gamma p}$, as a function of W for $Q^2 = 2.4\ GeV^2$ (dots) shown together with previous ZEUS measurements (squares) [18]. Also shown at higher Q^2 are the new measurements at $W = 155\ GeV$ (dots). The solid lines are the results of a fit of the form $\sigma^{\gamma^* p \to \gamma p} \propto W^{\delta}$. The values of δ and their statistical uncertainties are given in the figure. The inner error bars represent the statistical uncertainty while the outer error bars the statistical and systematic uncertainties added in quadrature.*

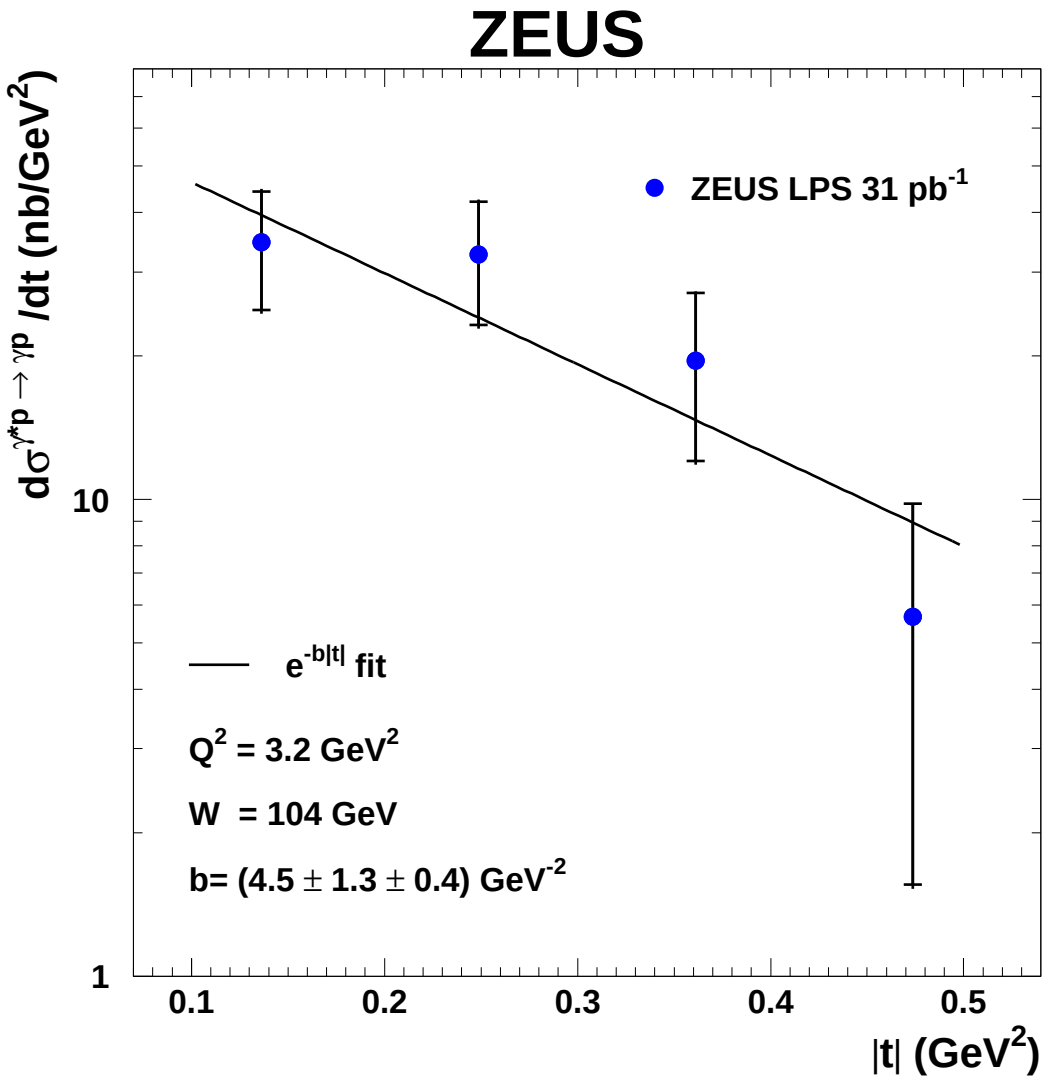

Figure 4: *The DVCS differential cross section, $d\sigma^{\gamma^* p \to \gamma p}/dt$, as a function of $|t|$. The solid line is the result of a fit of the form $\sim e^{-b|t|}$. The inner error bars represent the statistical uncertainty while the outer error bars the statistical and systematic uncertainties added in quadrature.*

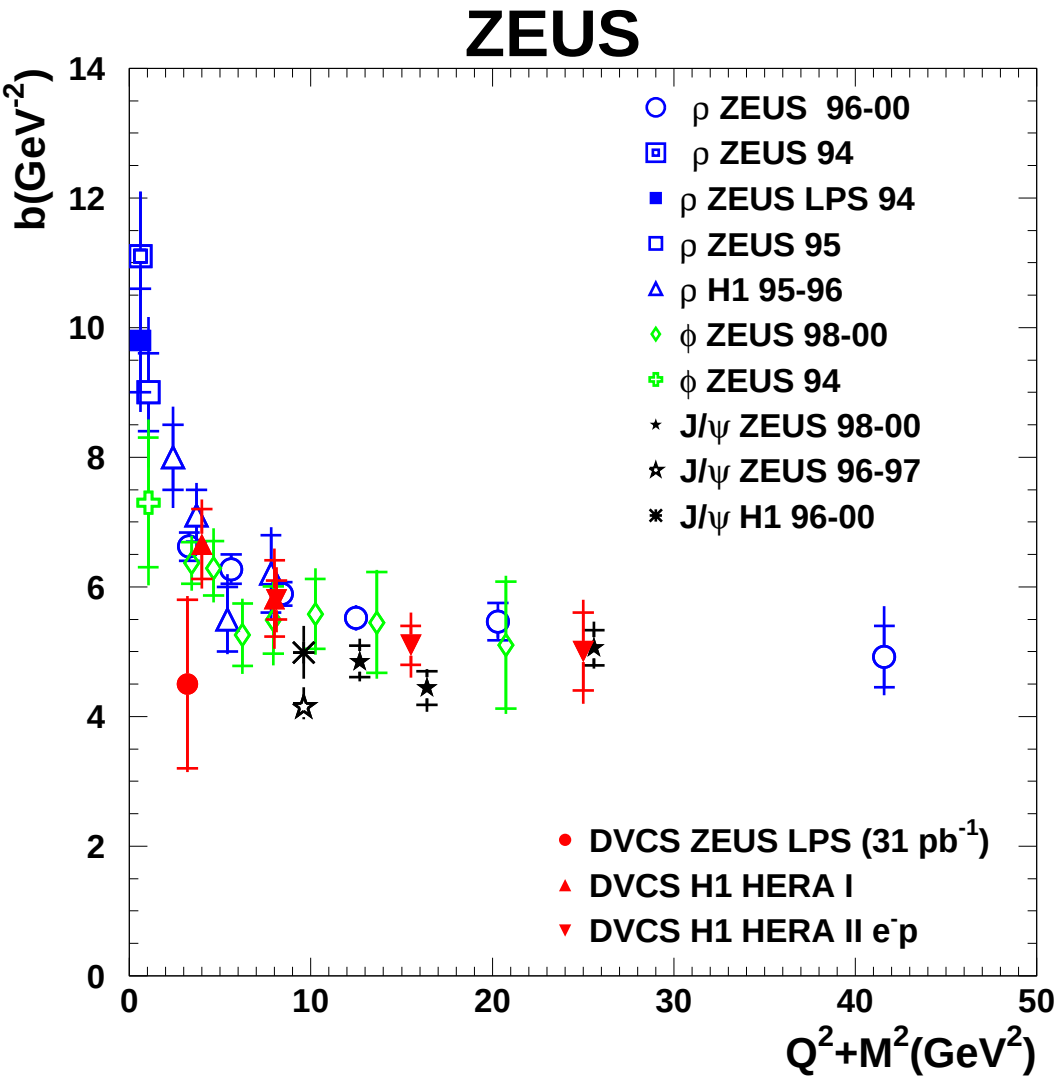

Figure 5: *A compilation of the values of the slope b as a function of $Q^2 + M^2$ for various exclusive processes including the present DVCS measurement. The inner error bars represent the statistical uncertainty while the outer error bars the statistical and systematic uncertainties added in quadrature.*